Effects of permeating ions and cGMP on gating and conductance of rod-type cyclic nucleotide-gated (CNGA1) channels

Jana Kusch, Vasilica Nache and Klaus Benndorf

Institut für Physiologie II, Friedrich-Schiller-Universität Jena, 07740 Jena, Germany

Cyclic nucleotide-gated (CNG) channels are tetrameric non-specific cation channels. They mediate the receptor potentials in photoreceptors and cells of the olfactory epithelium and they are activated by the binding of cyclic nucleotides such as cGMP and cAMP. Previous studies in homotetrameric CNGA1 channels, activated with covalently bound cGMP, presented evidence that partially liganded channels cause partial channel opening (Ruiz & Karpen, 1997, 1999). Here, homotetrameric CNGA1 channels were expressed in *Xenopus* oocytes. Conductance and gating of these channels were studied as a function of the concentration of freely diffusible cGMP and with different permeating ions. At saturating cGMP the current levels distributed around a single mean in a Gaussian fashion and the open times were long. At low cGMP, however, the current levels were heterogeneous: they were smaller than those at saturating cGMP, equal, or larger. The open times were short. Ions generating the larger single-channel currents ($Na^+ > K^+ > Rb^+$) concomitantly increased the heterogeneity of current levels and decreased the open probability and open times. The results suggest that the activation of CNGA1 channels by cGMP and ions staying longer in the pore is associated with less extensive and less frequent conformational fluctuations of the channel pore.

(Received 16 June 2004; accepted after revision 10 August 2004; first published online 12 August 2004)
Corresponding author K. Benndorf: Institut für Physiologie II, Friedrich-Schiller-Universität Jena, 07740 Jena, Germany. Email: klaus.benndorf@mti.uni-jena.de

Cyclic nucleotide-gated (CNG) channels (Kaupp *et al.* 1989) are non-specific cation channels, which are important for phototransduction in rod and cone photoreceptors and chemotransduction in olfactory cells (for review see Zimmerman, 1995; Finn *et al.* 1996; Kaupp & Seifert, 2002). Native CNG channels form heterotetramers composed of different subunits (Chen *et al.* 1993; Körschen *et al.* 1995; Bönigk *et al.* 1999; Zheng *et al.* 2002; Weitz *et al.* 2002; Zhong *et al.* 2002). Each subunit of CNG channels contains six transmembrane-spanning regions (S1–S6), a pore region between the S5 and S6 segment, and a cyclic nucleotide-binding domain (cNBD) in the C-terminus that is connected via the C-linker to the S6 segment (for review see Finn *et al.* 1996; Kaupp & Seifert, 2002). The binding of cyclic nucleotides to the cNBD is thought to trigger an allosteric change of conformation which leads to the opening of the pore. In the allosteric transition, multiple channel regions are involved. These include the C-linker and also remote areas with respect to the pore, such as the N-terminus and the S1–S2 region (Gordon & Zagotta, 1995; Möttig *et al.* 2001).

When studying basic functional properties of CNG channels, homomultimeric channels, expressed in appropriate heterologous cells, are often used because they comprise a defined composition. Gamel & Torre (2000) reported that Na^+ and K^+ ions modulate the channel gating in homomultimeric CNGA1 channels (for nomenclature see Bradley *et al.* 2001; Kaupp & Seifert, 2002). Recently, Holmgren (2003) studied the effect of permeating Na^+ and K^+ ions on the gating of CNGA1 channels at the single-channel level: at cGMP concentrations generating large open probability (P_o), intracellular K^+ caused higher P_o than intracellular Na^+ by prolonging the open channel lifetime. The author presented evidence that this effect is mediated by the interaction of the permeating ions with the pore. This interpretation is consistent with the idea that the selectivity filter of the CNG channel pore takes part in the gating (Sun *et al.* 1996; Bucossi *et al.* 1997; Becchetti *et al.* 1999; Liu & Siegelbaum, 2000; Flynn & Zagotta, 2001; Tränkner *et al.* 2004).

At cGMP concentrations generating low P_o and with Na^+ as permeating ion, native CNG channels produce

 DOI: 10.1113/jphysiol.2004.070193

sublevel openings (Hanke *et al.* 1988; Ildéfonse & Bennett, 1991; Taylor & Baylor, 1995). These results suggest that partial liganding at low cGMP promotes partial channel gating whereas full liganding at saturating cGMP promotes gating to the fully open channel. Further support for this hypothesis comes from results in homomultimeric CNGA1 channels locked in different ligand-bound states: with Na^+ as permeating ion, two sublevels were observed and their amplitude was attributed to the number of cGMP molecules bound to the channel (Ruiz & Karpen, 1997, 1999). These authors also presented evidence that low concentrations of freely diffusible cGMP generate respective sublevels. In contrast, with K^+ as permeating ion and freely diffusible cGMP the fully open level prevails at both saturating *and* low cGMP (Benndorf *et al.* 1999). These results show that the incidence of sublevels does not strictly depend on the cGMP concentration but also on the type of permeating ion. Hence, the permeating ions modulate P_o not only by altering the lifetime in the fully open state but also by affecting the channel conductance.

In this study, we have examined systematically the influence of cGMP and permeating ions on CNGA1 channel gating and conductance. We show that saturating cGMP generates long openings with a single current level, whereas low cGMP generates short openings with multiple current levels, including sublevels, the level observed at saturating cGMP, and superlevels. Ions that stay in the pore longer ($Rb^+ > K^+ > Na^+$) prolong the open times and decrease the multiplicity of current levels compared to ions staying in the pore for shorter times. The results suggest that at low cGMP the pore conformation fluctuates rapidly between multiple states of which some are open, whereas at saturating cGMP, the frequency and extent of the conformational fluctuations are strongly reduced. Permeating ions modulate these conformational fluctuations.

Methods

Oocyte preparation and cRNA injection

Ovarian lobes from female *Xenopus laevis* were resected under anaesthesia (0.3% 3-aminobenzoic acid ethyl ester) and transferred to a Petri dish containing Barth's medium (mM: 84 NaCl, 1 KCl, 2.4 $NaHCO_3$, 0.82 $MgSO_4$, 0.33 $Ca(NO_3)_2$, 0.41 $CaCl_2$, 7.5 Tris, pH = 7.4 with HCl). The individual donor animals were used four or five times. The condition of the animals was monitored between the ovarian lobe resections and care was taken to avoid distress or infection. The procedures had approval from the authorized animal ethical committee of the Friedrich Schiller University Jena. The animals were finally killed by decapitation under anaesthesia. The oocytes were treated for 60–90 min with 1.2 mg ml^{-1} collagenase (Type I, Sigma, St Louis, USA) and manually dissected. They were injected with 40–70 nl of a solution containing cRNA specific for CNGA1 channels (accession number X51604). The oocytes were incubated at 18°C in Barth's medium until experimental use within 6 days after injection.

Recording technique

The oocytes were positioned in the experimental chamber (volume 0.2 ml) mounted on the stage of an inverted microscope. Currents were recorded in inside-out patches with a patch-clamp technique. CNGA1 channels were activated with either 1.3, 10, 30, 100 or 700 μM cGMP. The concentration of 700 μM cGMP was used to maximally activate the channels (saturating cGMP). Each excised patch was first exposed to zero cGMP, to test for possible background channel activity, and then to saturating cGMP, to determine the maximum current. Patches with background channel activity were discarded. Three solutions were used: K^+ solution (mM: 150 KCl, 1 EGTA, 5 Hepes, pH = 7.4 with KOH), Na^+ solution (mM: 150 NaCl, 1 EGTA, 5 Hepes, pH = 7.4 with NaOH), and Rb^+ solution (mM: 150 RbCl, 1 EGTA, 5 Hepes, pH = 7.4 with RbOH).

The patch pipettes were pulled from either borosilicate glass tubing (outer diameter 2.0 mm, inner diameter 0.48 mm) or quartz tubing (outer diameter 1.2 mm, inner diameter 0.4 mm) on a laser puller (P-2000, Sutter Instrument Co., USA). The pipette resistances were 5–25 MΩ and 10–25 MΩ, respectively. The borosilicate glass pipettes were coated with Sylgard 184 (Dow Corning Corp., Midland, MI, USA) and fire-polished after coating.

Recording was performed with an Axopatch 200A amplifier (Axon Instruments, USA). The currents were on-line filtered (4-pole Bessel) at a cut-off frequency of 5 kHz. The currents were measured at the voltage of +100 mV to obtain reasonably large amplitudes of single-channel currents and to minimize proton block from the extracellular side, as demonstrated for structurally related CNGA2 channels (Root & MacKinnon, 1994). All measurements were performed at room temperature (22–24°C).

Data acquisition

Measurements were controlled and data were collected with the ISO2 soft- and hardware (12-bit resolution; MFK Niedernhausen, Germany) in conjunction with a Pentium PC. All currents were corrected for capacitive and very small leak components by subtracting corresponding averaged currents in the absence of cGMP. The sampling rate was generally 20 kHz.

Data analysis

If not otherwise indicated the recordings were off-line filtered to 2 kHz using a Gaussian algorithm. The amplitude of the single-channel currents was determined

by forming all-point amplitude histograms and fitting the distribution with sums of two Gaussian functions. At saturating cGMP, patches containing one and only one channel were used whereas at low cGMP, multichannel patches were used. Since the amplitude of single-channel currents at low cGMP varied considerably, the amplitude was determined from individual openings and only openings longer than 0.33 ms were included.

The single-channel open time was evaluated by setting a threshold to the 50% level of the current amplitude. At saturating cGMP the procedure was standard because only one level was present. At low cGMP the openings with different amplitudes were grouped to classes of 0.5 pA width and analysed in these classes. Cumulative open-time histograms were formed as the number of openings still open after time t given that all openings started at time zero. To reduce the variability, the open times of three to six patches were lumped by normalizing the histograms of an individual patch j with respect to the total time interval t_{tj}, from which the openings were included, and summing up these values. The cumulative open-time histograms for m patches were finally plotted in the form:

$$\frac{1}{N}\sum_{j=1}^{m}\frac{(\text{No. of openings still open at } t \mid \text{ open at } t=0)_{\text{i}}}{t_{tj}}$$

where N is the total number of channels in all j patches. N was determined for each patch by $N = I_{\text{sat}}/i$ where I_{sat} and i are the amplitudes of the multichannel current (700 μM) and of the single-channel current at saturating cGMP as determined from single-channel patches, respectively. The cumulative open-time histograms were fitted with either a single exponential

$$y(t) = A_{\text{f}}\exp(-t/\tau_{\text{of}}) \tag{1a}$$

or in the case of an additional slow component with the sum of two exponentials

$$y(t) = A_{\text{f}}\exp(-t/\tau_{\text{of}}) + A_{\text{s}}\exp(-t/\tau_{\text{os}}). \tag{1b}$$

τ_{of}, τ_{os}, A_{f} and A_{s} are the fast and the slow open-time constants and their relative contributions, respectively. The open probability, P_{o}, for the events included in each histogram was obtained by integrating eqns (1a) or (1b) within the limits 0 and ∞ yielding

$$P_{\text{o}} = A_{\text{f}}\tau_{\text{of}} \tag{2a}$$

$$P_{\text{o}} = A_{\text{f}}\tau_{\text{of}} + A_{\text{s}}\tau_{\text{os}}. \tag{2b}$$

Determining P_{o} in this way includes an estimated value for the missed brief events.

Because the amplitudes of the single-channel currents were heterogeneous, the probability that an apparently single-channel event was composed of the events of two channels was considered: the expression level was chosen such that at each cGMP concentration tested the fraction of events generated by an obvious overlap of two events was below 10%. These events, as identified by the presence of more than one level or a shoulder in the rising or falling phase, were excluded from the analysis. We then estimated the probability that an apparent single-channel event was composed of two overlapping smaller events in which both opening transitions occurred simultaneously and both closing transitions occurred simultaneously. This probability is the product of the probabilities of a simultaneous opening transition, P_{so}, and of a simultaneous closing transition, P_{sc}. Two opening or closing transitions were considered to be non-separable if they occurred within one 10–90% rise time, $t_{\text{r}} = 0.3321/f_{\text{c}}$ (Benndorf, 1995), where f_{c} is the cut-off frequency of the filter. With $f_{\text{c}} = 2$ kHz, t_{r} was 166 μs. The trace duration t_{d} was 400 ms and the average number of apparent single-channel events per 400 ms trace, x_n, ranged from 2.0 to 45.0. The probability of a simultaneous transition of two channels from a closed to an open state, P_{so}, was estimated by

$$P_{\text{so}} = x_n t_{\text{r}}/t_{\text{d}}. \tag{3}$$

With eqns (1) and (2) the probability that two channels close in the time interval t to $t + t_{\text{r}}$, given that they opened at $t = 0$, is

$$P_{2\text{c}(t,t+t_{\text{r}})} = \left[-(A_{\text{f}}\tau_{\text{of}} + A_{\text{s}}\tau_{\text{os}})^{-1}\int_{t}^{t+t_{\text{r}}} y(t)\,\text{d}t\right]^2. \tag{4}$$

The total probability that two channels close in the same time interval t to $t + t_{\text{r}}$ for $t \geq 0.33$ ms (openings shorter than 0.33 ms were excluded), given that they opened at $t = 0$, is then

$$P_{\text{sc}} = \sum_{j=0}^{\infty} P_{2\text{c}[2+jt_{\text{r}},2+(j+1)t_{\text{r}}]}. \tag{5}$$

Practically, the sum was calculated until $t_{\text{d}}/t_{\text{r}}$. The probability to mistake the superimposition of two events with simultaneous opening and closing as a single event is then

$$P_{\text{mis}} = P_{\text{so}}P_{\text{sc}}. \tag{6}$$

Curve fits and statistics

Curves were fitted to the data with appropriate non-linear approximation algorithms using either the ISO2 or the Origin 6.1 software. Statistical data are given as mean ± S.E.M. For open-time histograms constructed from the events of all patches, the error of the fits refers to the 95% confidence interval limit provided by the Origin 6.1 software.

Results

At saturating cGMP the channels generate a single current level

Figure 1*A* shows representative single-channel currents of CNGA1 channels at saturating cGMP with symmetrical Na^+ or K^+ ions. In the presence of either ion, single-channel currents with one level were observed. Amplitude histograms show that the single-channel currents were 1.8 times larger for Na^+ than for K^+ currents (Fig. 1*B* and Table 1). The fit of the open-time histograms yielded a fast and a slow time constant, τ_{of} and τ_{os}, respectively. Both time constants were significantly smaller for Na^+ than for K^+ ions (Fig. 1*C* and Table 1). Because P_o was similar (Table 1), it follows that the channel fluctuates more frequently between the closed and the open state in the presence of Na^+ ions. These results confirm observations by Holmgren (2003).

Figure 1*B* also shows that the open level distributions are wider than the closed level distributions. One source of this open-channel excess noise is conformational fluctuations of the channel pore, as shown for acetylcholine receptor currents (Sigworth, 1985). In CNGA2 channels, a block of the pore by external protons also contributes to the excess noise (Root & MacKinnon, 1994). In the present study this block should be only low because the voltage was generally set to the very positive value of +100 mV and the pH was 7.4. We therefore assumed that the excess noise is essentially generated by differences in the conformational fluctuations of the pore. The excess noise of the open channels is described by

$$\sigma_{nx} = \left(\sigma_{ox}{}^2 - \sigma_c{}^2\right)^{1/2} \quad (7)$$

where σ_{ox} and σ_c are the root mean square (RMS) noise of the xth open level and the closed level, respectively (Fig. 1*B*). The excess open-channel noise was larger for Na^+ than for K^+ ions (Table 1). However, after normalization with respect to the single-channel current, σ_{n1} was similar for both ions (Table 1). This result suggests that at saturating cGMP the amplitude of the conformational fluctuations of the open pore does not depend on the ion species.

At low cGMP the channels generate multiple current levels

At 10 μM cGMP, only a small fraction of current is activated (K^+_i/K^+_o: $I/I_{max} = 5.7 \times 10^{-3}$; Na^+_i/Na^+_o: $I/I_{max} = 2.6 \times 10^{-3}$). At this low cGMP concentration the amplitudes of the single-channel currents were heterogeneous in the presence of either ion, being either smaller (sublevels) or larger (superlevels) with respect

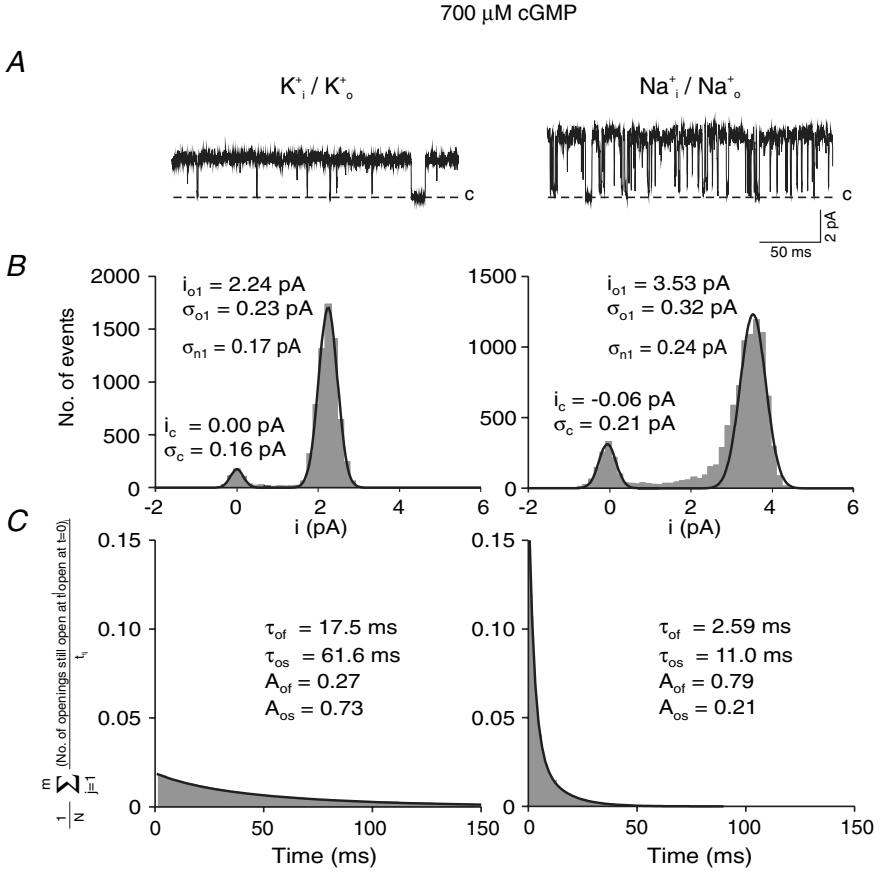

Figure 1. Single CNGA1 channel currents at saturating cGMP (700 μM) with either symmetrical Na^+ or K^+ ions at +100 mV
A, current traces. K^+ ions produced openings smaller in amplitude, longer in duration, and with a less noisy open level compared to Na^+ ions. *B*, amplitude histograms. All-point histograms were fitted with the sum of two Gaussian functions yielding the indicated values for the mean (i_{o1}, i_c) and standard deviation (σ_{o1}, σ_c) at the open and closed levels, respectively. σ_{n1} indicates the extra RMS noise of the open channel calculated using eqn (7). *C*, cumulative open-time histograms. The histograms were fitted with eqn (1b) yielding the indicated parameters. Both open time constants are shorter for Na^+ than for K^+ currents.

Table 1. Single-channel parameters at saturating cGMP (700 μM) for Na^+ and K^+ currents at +100 mV

	K^+_i/K^+_o	Na^+_i/Na^+_o
i (pA)	2.0 ± 0.13 (10)	3.6 ± 0.17 (6)
σ (pA)	0.20 ± 0.013 (3)	0.33 ± 0.015 (3)
σ/i	0.100 (3)	0.092 (3)
P_o	0.94 ± 0.024 (4)	0.81 ± 0.030 (3)
τ_{of} (ms)	17.5 ± 1.09 (312)*	2.59 ± 0.04 (307)*
τ_{os} (ms)	61.9 ± 0.69 (312)*	11.0 ± 0.30 (307)*
A_f	0.27 ± 0.016 (312)*	0.79 ± 0.015 (307)*
A_s	0.73 ± 0.026 (312)*	0.21 ± 0.011 (307)*

i, amplitude of the single-channel current; P_o, open probability; σ_{n1}; RMS noise of the open level determined with eqn (7); σ_{n1}/i, RMS noise of the open level normalized with respect to i; τ_{of}, fast open time constant; τ_{os}, slow open time constant; A_f, amplitude of the fast component of the open time; A_s, amplitude of the slow component of the open time. The numbers in parentheses indicate the number of patches or the number of individual openings (*) included in the statistics.

to the level observed at saturating cGMP (Fig. 2*A*). Closer inspection of all traces revealed openings to many different levels from just detectable sublevels to the largest superlevels (Fig. 2*B*).

Because these measurements involved multichannel patches, we estimated the probability P_{mis} to mistake the superimposition of two distinct events with simultaneous opening *and* simultaneous closing as a single event (see Methods). The values of P_{mis} determined for the individual patches ranged from 6.9×10^{-6} to 4.8×10^{-4}, i.e. in the worst case, only one out of 2083 openings might have been identified as false positive. Therefore, all openings, were considered as originating from a single channel.

Amplitude histograms of the single-channel events were constructed to evaluate the incidence of current levels. To obtain maximum resolution, only time intervals were included when a channel was open, i.e. all closed level and all transition points were excluded. The distributions (grey areas in Figs 3 and 4) were fitted with sums of Gaussian functions providing respective means, i_x. Figure 3*A* shows amplitude histograms for Na^+ currents from three patches at 10 μM cGMP. The openings are grouped with respect to two or three means. The distributions are significantly different from patch to patch, although the experimental conditions were identical. In patches 1 and 2, most of the events were sublevel compared to the current level observed at saturating cGMP (dotted vertical line), whereas in patch 3 two large Gaussians were positioned at both sides of this level. In patches 2 and 3, a noticeable fraction of events were superlevels.

The histograms also provide the extra noise, σ_{nx}, for the xth open level calculated by eqn (7). The values of σ_c (not shown) were calculated from baseline noise obtained from time intervals with no channel opening (open areas). Most of the σ_{nx} values were larger than that at saturating cGMP (0.33 ± 0.015 pA). A wider Gaussian distribution can be either the result of larger open-channel noise or a larger heterogeneity of current levels. In the first case, the conformational fluctuations of the pore that cause this noise are fast compared to the range of open times, whereas in the second case the conformational fluctuations of the pore are slow compared to this time range. The observed multitude of current levels (Fig. 2*B*) suggests that slow conformational fluctuations have caused the larger noise in the Gaussian components at low cGMP. Although the reason for the remarkable heterogeneity of the amplitude distributions among the patches is presently not clear, these results show that the individual Gaussian components are

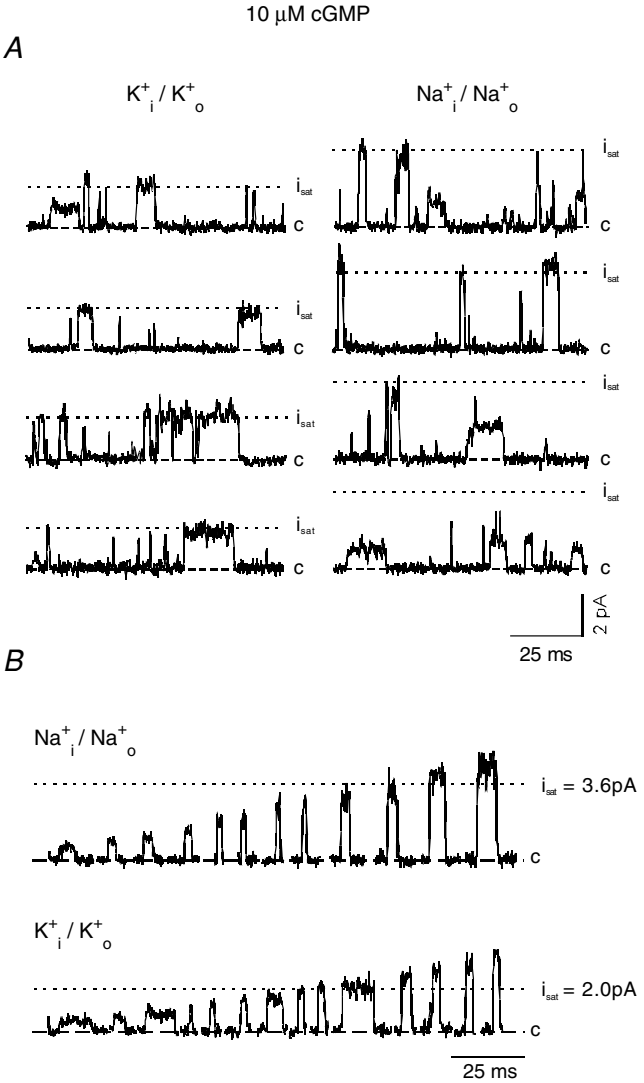

Figure 2. Single CNGA1 channel currents at low cGMP (10 μM) with either symmetrical Na^+ or K^+ ions
The dotted lines indicate the current level observed at saturating cGMP (700 μM; see Fig. 1). *A*, representative current traces. Openings to sublevels, the level observed at saturating cGMP, and superlevels appeared with both ions. *B*, selected openings in order of amplitude.

not related to the number of bound ligands in a simple fashion.

Figure 3*B* shows amplitude histograms of Na^+ currents at 30 μM cGMP. As at 10 μM cGMP, the amplitude distributions differed substantially between the patches. Also the excess noise (σ_{nx}) was heterogeneous, being smaller and larger than that at saturating cGMP. Despite this heterogeneity, the distributions tend to group more closely to the level observed at saturating than at 10 μM cGMP. We interpret this result to indicate that cGMP reduces slow conformational fluctuations of the channel pore with respect to the range of open times.

Figure 4 shows similar experiments with K^+ currents. At 10 μM cGMP, the channel activity was primarily represented by a single, large Gaussian distribution that peaked either directly (patches 4 and 6) or close (patch 5) to the level determined at saturating cGMP (Fig. 4*B*). A second Gaussian with a smaller mean contributed minimally in all patches. The means varied between the patches. The excess noise of the large Gaussians (σ_{n2}) always exceeded that at saturating cGMP (0.20 ± 0.013 pA), suggesting that it is the different levels (Fig. 2*B*) that generate the wider distributions.

Figure 4*A* shows respective amplitude histograms at 1.3 μM cGMP. Comparison of the histograms at 1.3 μM cGMP and 10 μM cGMP confirms that the higher cGMP concentration confines the current levels closer to the level observed at saturating cGMP by two effects: the excess noise of the prevailing Gaussian and the contribution of the sublevel events are smaller at 10 than at 1.3 μM cGMP. Hence, also in the presence of K^+ ions a higher cGMP concentration reduces slow conformational fluctuations of the channel pore.

We next considered whether the different amplitude distributions with Na^+ and K^+ at the same low cGMP concentration (Figs 3*A* and 4*B*) are due to a different P_o or to specific effects of the ions, independent of P_o. We therefore compared amplitude distributions with Na^+ ions at a slightly larger P_o to those with K^+ ions at a respective lower P_o (compare Fig. 3*B*, Na^+: $P_o = 9.1 \times 10^{-3}$, to Fig. 4*B*, K^+: $P_o = 5.2 \times 10^{-3}$; and Fig. 3*A*, Na^+: $P_o = 3.4 \times 10^{-3}$, to Fig. 4*A*, K^+: $P_o = 9.6 \times 10^{-4}$). These comparisons illustrate that K^+ ions stabilize the current level observed at saturating cGMP with respect to Na^+ ions independent of P_o.

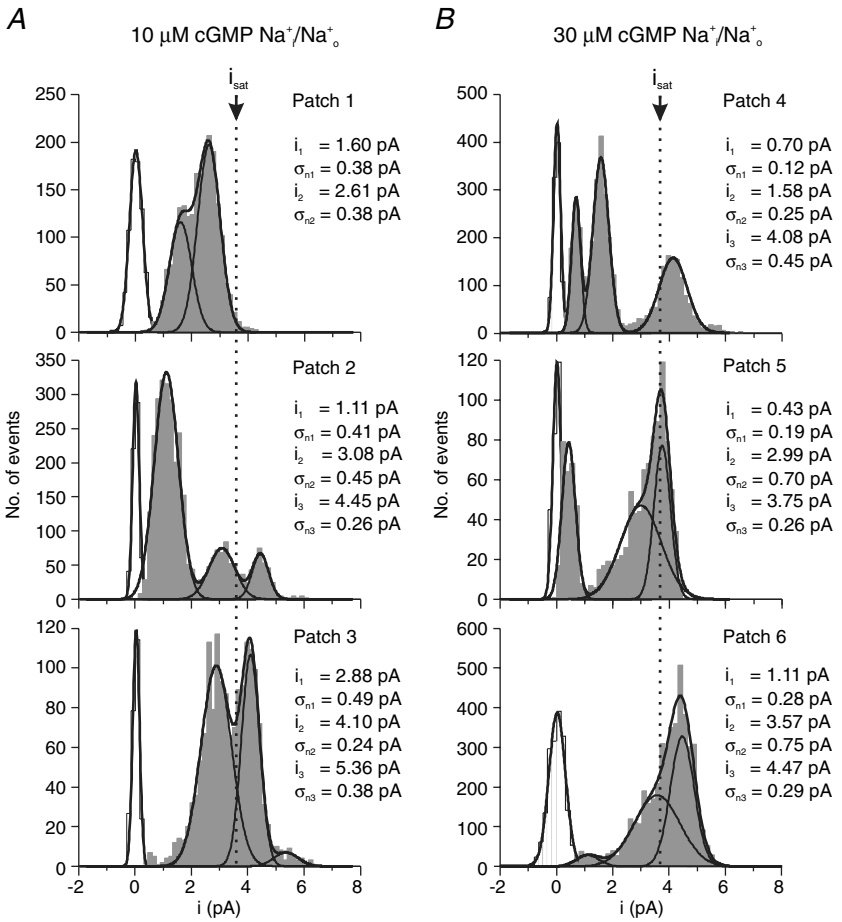

Figure 3. Amplitude histograms of single-channel openings with Na^+_i/Na^+_o recorded from six patches
Transition and baseline points were removed. Filter, 2 kHz. The distributions were fitted by sums of Gaussian functions. For each Gaussian curve the mean (i_x) and the open-channel RMS noise (σ_{nx}) is indicated. σ_{nx} was calculated according to eqn (7). The dotted line indicates the current level observed at saturating cGMP. The baseline peaks (open) were calculated separately from time intervals in the absence of channel activity. *A*, 10 μM cGMP. The histograms of the patches show either two or three Gaussian distributions. *B*, 30 μM cGMP. As at 10 μM cGMP the distributions differ notably but tend to shift more to i_{sat}.

Effects of Na^+ and K^+ ions on open times and P_o at low cGMP

At high cGMP concentrations, Na^+ ions destabilize the open channel with respect to K^+ ions by decreasing the mean open time (Holmgren, 2003; Table 1). We examined whether Na^+ ions also exert similar effects at low cGMP and therefore analysed the open times for both ions over a wide range of cGMP concentrations.

Because of the heterogeneity of the current levels, the opening events were grouped into amplitude classes of 0.5 pA width and for each 0.5 pA class, cumulative open-time histograms were formed (Methods). Figure 5*A* shows these histograms for all occupied classes at 10 μM cGMP. The open times differ between the amplitude classes (for time constants see legend to Fig. 5*A*). A slow open time constant (τ_{os}) is present only with K^+ ions. Its contribution, however, significantly differs between the classes. These results indicate that different conductance states have different lifetimes and that K^+ ions prolong the lifetimes of the conductance states differently.

To obtain the cumulative open-time histogram for all current levels, the histograms of all occupied classes were summed (Fig. 5*B*). For both ions, these histograms required two exponentials for description. This analysis was also performed at other cGMP concentrations and the resulting open-time constants are shown in Fig. 6*A*. Both time constants are shorter with Na^+ than with K^+ ions at all cGMP concentrations and the shortening effect is stronger at high than at low cGMP.

We also determined the open probability P_o for all current levels. It was obtained from the area under the fitted curves in the summed cumulative open-time histograms (Fig. 5*B*). P_o was plotted as function of the cGMP concentration for both ions (Fig. 6*B*). K^+ ions produced a larger P_o than Na^+ ions at all cGMP concentrations and the effect of the ions was stronger at low than at high cGMP (for saturating cGMP see also Table 1).

Ions and cGMP modulate different closing reactions

We addressed the question of whether the ions and cGMP affect the same single closing reaction. Consider the effects of Na^+ and K^+ on P_o and τ_{of} at Na^+/700 μM cGMP and K^+/100 μM cGMP (Fig. 6, arrows). $P_o(K^+/100\,\mu M$ cGMP) is lower than $P_o(Na^+/700\,\mu M$ cGMP). If the lower $P_o(K^+/100\,\mu M$ cGMP) were caused solely by the same closing reaction accelerated at 100 μM cGMP

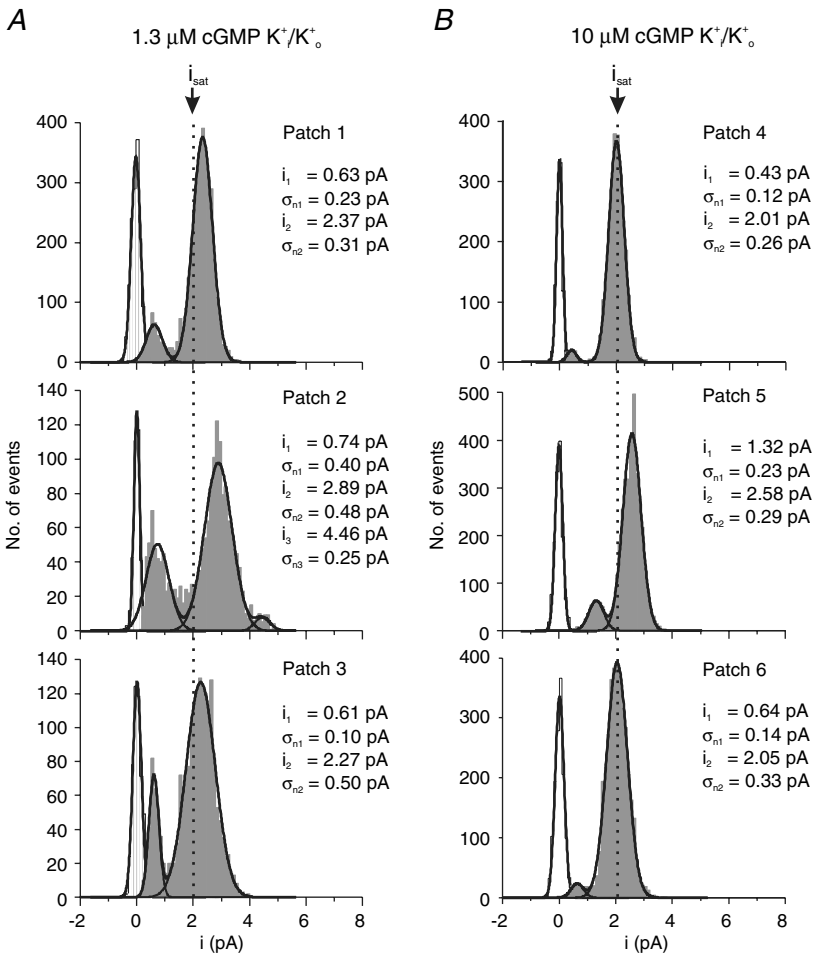

Figure 4. Amplitude histograms of single-channel openings with K^+_i/K^+_o recorded from six patches
For an explanation of conditions and symbols see Fig. 3. *A*, 1.3 μM cGMP. The histograms of the patches show either two or three Gaussian distributions. *B*, 10 μM cGMP. As at 1.3 μM cGMP, the distributions differ notably and they shift more to i_{sat}. The RMS noise of the main peaks (σ_{n2}) still exceeds that at saturating cGMP (Table 1).

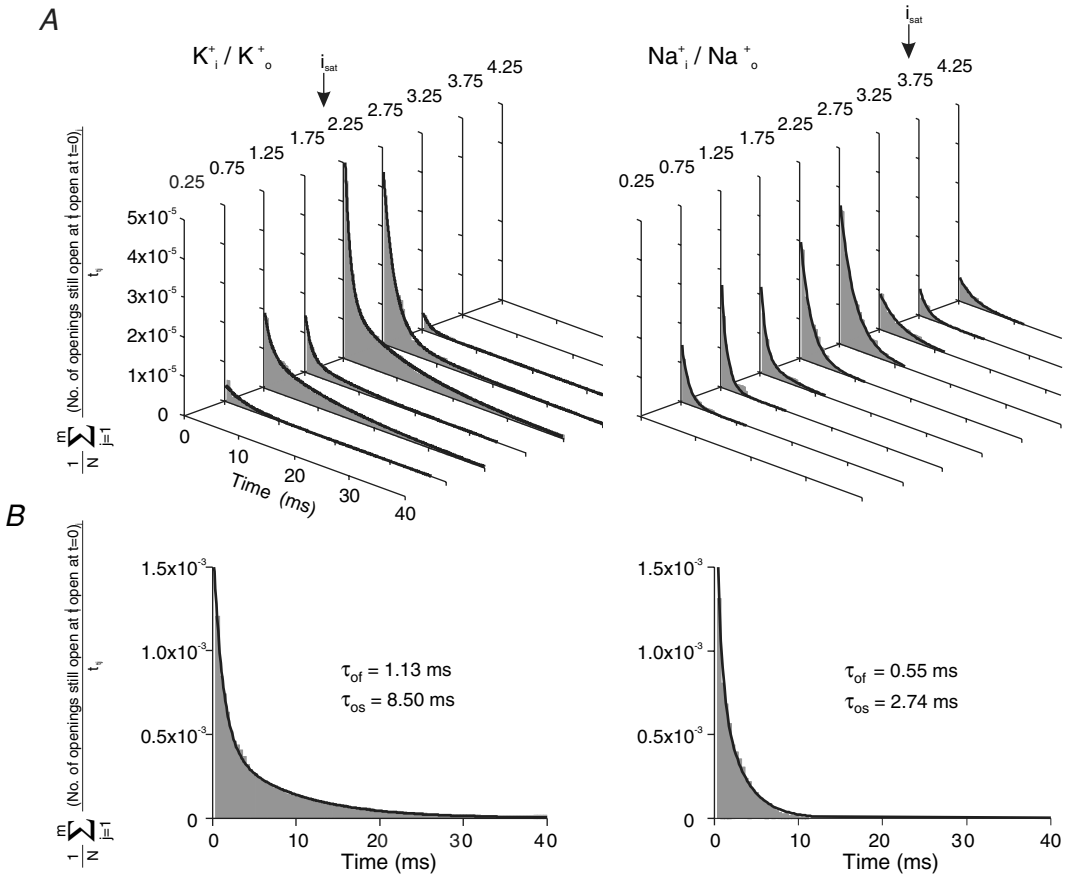

Figure 5. Cumulative open-time histograms for Na^+ and K^+ at 10 μM cGMP
A, histograms for amplitude classes of 0.5 pA width. The histograms were attributed to the class means and fitted with eqns (1a) or (1b). The areas under the curves indicate P_o within each class. The individual time constants were: K^+_i/K^+_o (for the class means 0.75 to 3.25 pA): $\tau_{of} = 3.32$ ms, $\tau_{of} = 1.26$ ms, $\tau_{os} = 11.1$, $\tau_{of} = 1.04$ ms, $\tau_{os} = 7.45$ ms, $\tau_{of} = 0.97$ ms, $\tau_{os} = 10.1$ ms, $\tau_{of} = 1.94$ ms, $\tau_{os} = 10.9$ ms, $\tau_{of} = 1.30$ ms. Na^+_i/Na^+_o (for the class means 0.75 to 4.25 pA): $\tau_{of} = 1.22$ ms, $\tau_{of} = 1.01$ ms, $\tau_{of} = 1.57$, $\tau_{of} = 1.93$ ms, $\tau_{of} = 2.60$ ms, $\tau_{of} = 3.30$ ms, $\tau_{of} = 1.46$ ms, $\tau_{of} = 2.50$ ms. *B*, cumulative histograms for all amplitude classes. The histograms were fitted with eqn (1a).

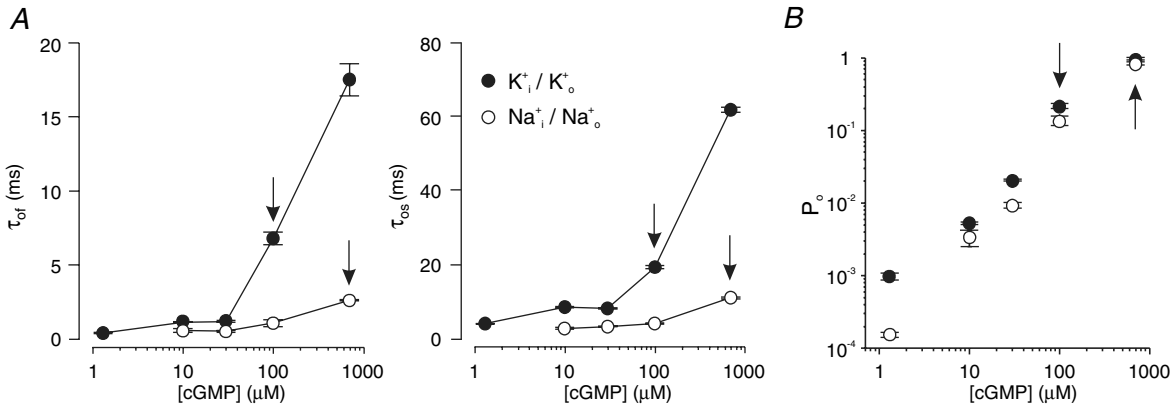

Figure 6. Effects of the permeating ions on single-channel parameters as a function of the cGMP concentration
A, open times. τ_{of} and τ_{os} denote mean fast and slow open times, respectively. With K^+ as the permeating ion, both open times were longer than with Na^+ as the permeating ion. *B*, open probability, P_o. The P_o values were determined from cumulative open-time histograms including the openings of all amplitude classes. Each histogram contains between 259 and 920 individual openings and each data point contains data from three to six patches.

compared to 700 μM cGMP, then τ_{of}(Na^+/700 μM cGMP) should be larger than τ_{of}(K^+/100 μM cGMP). Instead, τ_{of}(Na^+/700 μM cGMP) was smaller than τ_{of}(K^+/100 μM cGMP) (arrows in Fig. 6*A*, left). Similar results were obtained with other pairs of neighboured cGMP concentrations and also when τ_{os} was considered instead of τ_{of} (arrows in Fig. 6*A*, right). We therefore conclude that at least two reactions determine the channel closure and that the ions modulate the contributions of these reactions.

Ions permeating the pore more slowly stabilize the open channel

The smaller single-channel current with K^+ than with Na^+ suggests that K^+ ions bind longer to a binding site within the pore than Na^+ ions. If the longer binding of K^+ ions to the binding site is also responsible for the lower heterogeneity of single-channel current amplitudes and the longer open times, then ions generating even smaller single-channel current than K^+ ions should further reduce the heterogeneity of current levels and increase the open times. Such small single-channel currents were reported with Rb^+ ions (Nizzari *et al.* 1993) and for structurally related voltage-gated K^+ channels it has been shown that Rb^+ ions stay longer in the channel than K^+ ions (Swenson & Armstrong, 1981). We recorded Rb^+ currents at cGMP concentrations between 10 and 700 μM. Because of the small amplitude of the currents, the analysis was performed at a band width of 300 Hz. To additionally prove that it is the intracellular and thus the permeating ions which cause the effects on gating, Rb^+ and K^+ currents were recorded with Na^+ ions at the extracellular side.

The traces in Fig. 7*A* show that at 700 μM cGMP Rb^+ ions generated an 'always-open' channel. At 30 μM cGMP, the open level was the same as at saturating cGMP and openings to sub- or superlevels were either absent or only extremely rare (Fig. 7*B*). This result differs from that with permeating K^+ ions (Fig. 7*C*) and even more from that with permeating Na^+ ions at 30 μM cGMP (cf. Fig. 3*B*). Rb^+ currents showed a noticeable heterogeneity of current levels only at the low cGMP concentration of 10 μM and, as expected, Rb^+ increased both open times (Fig. 7*D*) with respect to K^+. Together, these results confirm the above hypothesis that ions staying longer in the pore stabilize the open channel by two mechanisms, by reducing the number of accessible conformational states of the pore and decelerating the channel closure.

Discussion

In this study we reconsidered the gating of single homomultimeric CNGA1 channels as a function of the cGMP concentration and the type of permeating ion. Our results demonstrate that an increased cGMP concentration correlates not only with higher P_o and longer open times but also with a decreased incidence of heterogeneous current levels. Ions staying longer in the pore affect these functional parameters similarly but the extent of these ionic effects is smaller than that of the cyclic nucleotide. Because the selectivity filter is the principal gate for the cyclic nucleotide-induced gating (Sun *et al.* 1996; Bucossi *et al.* 1997; Becchetti *et al.* 1999; Liu & Siegelbaum, 2000; Flynn & Zagotta, 2001) and the ions affect the gating when permeating the pore (Fig. 7; cf. Holmgren, 2003), all gating effects described in this paper can be attributed to conformational changes of the channel pore.

The pronounced heterogeneity of current levels at low cGMP (low P_o) indicates that the pore conformation can adopt multiple open states. The individual events, however, contained mostly only a single level, even in multichannel patches. This result shows that the switching of the channel to the next conductance state must proceed when the channel pore is closed. It is therefore likely that the pore passes at least two closed states between two open states with different conductance. The fact that at low P_o the sojourns of the pore in closed states are much longer than those in open states makes it likely that even more closed states are passed between two open states. It is therefore suggested that at low P_o the pore conformation fluctuates between multiple states of which only a small fraction is open. The conductance of these open states can be different, generating the heterogeneity of current levels.

At saturating cGMP, the absence of heterogeneous current levels indicates that the high concentrations of the bound cyclic nucleotide prevents the pore from adopting most of the open pore conformations in the sense that the pore is 'frozen' in conformations generating only one conductance. Because of the biexponential distributions of the open times, there are at least two open pore conformations. The effect of increasing the cGMP concentration on the pore can therefore be understood as a reduction of the number of accessible states. The high P_o suggests that the accessibility of closed states is significantly more reduced than that of the open states. A cGMP-induced reduction of the number of accessible closed and open states can also explain the longer open times at high than at low cGMP: with fewer accessible states at high cGMP, fewer transitions are possible along which an open state can be left. Hence, increasing cGMP does not only reduce the extent of conformational pore fluctuations, as suggested by a reduced number of current levels, but also the frequency of these fluctuations, as suggested by the longer open times.

The effect of the permeating ions on the gating is also directed on the conformational fluctuations of the pore; ions staying longer in the pore ($Rb^+ > K^+ > Na^+$) exert similar effects to an increased cGMP concentration; at

low cGMP the number of accessible conductance states is reduced, P_o and the open times are increased. The effects of ions, however, are only weak compared to those of the cGMP concentration. The result that at saturating cGMP the heterogeneity of levels is lost with all ion species supports the notion that ions and cGMP control the extent of conformational fluctuations via the same mechanism. Despite this result, our data also suggest that ions and cGMP affect different closing reactions because the open times at saturating cGMP remain different with the different ions (Fig. 7*D*). This result supports the notion that ions and cGMP control the frequency of conformational fluctuations by involving different closing reactions. Evidence for different closing reactions affected by ions and cGMP was also derived above from the analysis of P_o and the open times (see text to Fig. 6).

We observed that the different amplitudes of the Rb^+, K^+ and Na^+ currents at saturating cGMP negatively correlate with the degree of heterogeneity of current levels and the prolongation of open times. From a mechanistic point of view it is likely that these effects of ions depend on the dwell time of the ions in the pore. With single-channel currents in the range of 0.5 pA (Rb^+) to 3.6 pA (Na^+), the upper limit of the mean dwell time of the ion in the channel is 3.2×10^{-7} to 4.5×10^{-8} s. Since these dwell times are much shorter than the open times, an ion binding

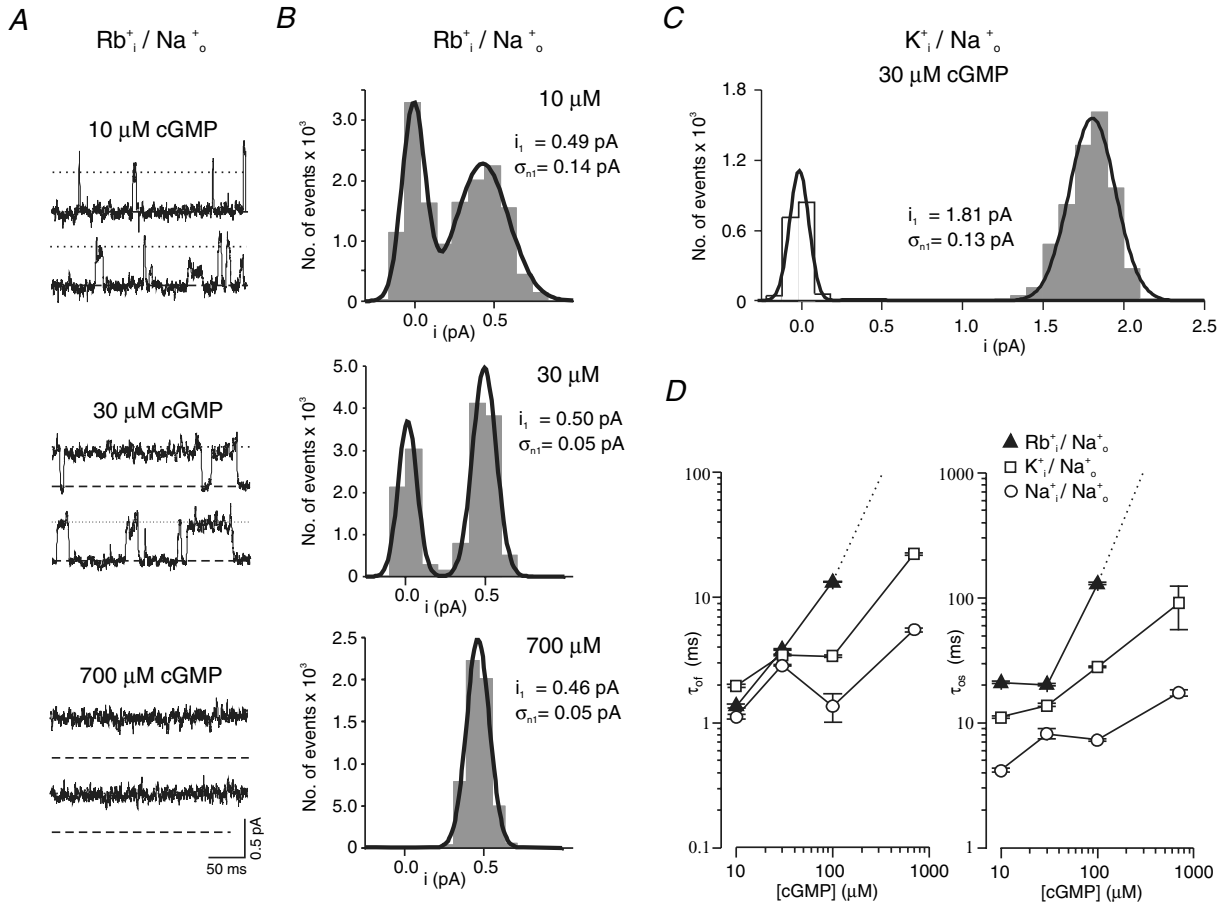

Figure 7. Effect of the permeant ions on channel gating
The pipettes contained Na^+ ions. The voltage was +100 mV. Filter, 300 Hz. *A*, single-channel Rb^+ currents recorded with 150 mM Rb^+ in the bath solution. At 700 μM cGMP the channel was nearly always open and generated only one level. At 30 μM cGMP the channel switched between the closed level and the level observed at saturating cGMP. In contrast, at the low concentration of 10 μM cGMP sub- and superlevels were observed in addition to the level observed at saturating cGMP (dotted lines). *B*, amplitude histograms for Rb^+ currents. At 10 μM cGMP the open level distribution was wider than at 30 or 700 μM cGMP. At the subsaturating cGMP concentrations, the histograms were formed from selected events of multichannel patches (see Methods). The excess noise (σ_{n1}) was calculated using eqn (7) from the noise of the open and the closed levels. For σ_{n1} at 700 μM cGMP, the noise of the closed level was determined in the absence of cGMP. *C*, amplitude histograms for K^+ currents (with Na^+ at the extracellular side). At 30 μM cGMP, the open level distribution was wider (larger σ_{n1} value) than at the same cGMP concentration with Rb^+ ions. *D*, plot of the fast and the slow open times, τ_{of} and τ_{os}, as a function of the cGMP concentration for Rb^+, K^+ and Na^+ ions. Rb^+ produced longer open times than K^+. The dotted lines indicate that at saturating cGMP the open times were too long for proper determination.

in the pore cannot stabilize the open channel directly by its dwell time at the binding site. One possible explanation is that several ions bind in the pore simultaneously and that channel closure is only possible when both (or all) binding sites are empty. Evidence for the simultaneous binding of two ions in the selectivity filter has been provided for K^+ channels (Doyle *et al.* 1998). Alternatively, it is conceivable that the mean time an ion occupies a single binding site is transformed to decreased conformational fluctuations of the pore region.

Gamel & Torre (2000) were the first to show that permeating ions modulate the gating of CNGA1 currents. Replacing Na^+ on the inside by K^+ slowed down the channel gating at positive voltages. This result fits with the idea derived from this study that K^+ ions reduce the frequency of conformational fluctuations with respect to Na^+ ions. Our results also confirm the previous results of Holmgren (2003) who observed at cGMP concentrations generating large P_o that permeating K^+ ions prolong the open-channel lifetime with respect to permeating Na^+ ions.

In previous work on the incidence of sublevel openings at low cGMP, Ruiz & Karpen (1997, 1999) reported that CNGA1 channels locked in partially liganded states with 8-p-azidophenacylthio- cGMP (APT-cGMP) produce distinct sublevels and the authors identified these sublevels also when activating the channels with free cGMP. With symmetrical Na^+ and at low cGMP we also observed a preference for sublevel openings but our amplitude histograms did not confirm the notion that partial liganding causes only partial opening (Figs 3 and 4). Generally, when relating results obtained with permanently bound APT-cGMP to those obtained with freely binding cGMP, one should be aware that this is only possible if the binding/unbinding reaction of the free cGMP is slow compared to the subsequent allosteric reaction. This has not been shown so far. If the allosteric reaction is slower than the binding reaction then the observed amplitude heterogeneity in our measurements (including the superlevels) could be lost in the experiments of Ruiz & Karpen simply by the permanent binding of the APT-cGMP. Hence, our results do not necessarily conflict with those of Ruiz & Karpen (1997, 1999) obtained with permanently bound APT-cGMP but reflect the channel action with freely diffusible cGMP.

The present data also explain contradictory results on the incidence of sublevels at partially activated CNGA1 channels in the studies of Ruiz & Karpen (1997, 1999) and our work (Benndorf *et al.* 1999): while Ruiz & Karpen (1999) reported that sublevel openings dominate the channel activity, we observed a mean current level close to the level observed at saturating cGMP (Benndorf *et al.* 1999). The results of this study show that permeating Na^+ ions particularly promote sublevels whereas permeating K^+ ions promote levels both smaller and larger than the level observed at saturating cGMP, resulting in amplitude histograms with an open-level distribution apparently close to that for the level observed at saturating cGMP. The fact that at very low P_o (1.3 and 10 μM cGMP; Fig. 6*B*) the channels generated not only sublevels but also the level observed at saturating cGMP and superlevels, rules out that a partially liganded channel produces a distinct subconductance state.

Native channels are heterotetramers composed of three CNGA1 subunits and one modulating CNGB1 subunit (Zheng *et al.* 2002; Weitz *et al.* 2002; Zhong *et al.* 2002). Two of the modulating effects of the CNGB1 subunit are to decrease the single-channel conductance and to increase the open-channel noise, if compared to homotetrameric CNGA1 channels (Körschen *et al.* 1995). In the context of the present study these results suggest that the CNGB1 subunit also modulates the conformational fluctuations of the channels. In future experiments it would be of interest to examine how this modulation is related to the effects of cGMP and the ions described here. Other interesting areas for further study are conformational fluctuations at physiological voltages and with physiological ions, including external Ca^{2+} ions. Ca^{2+} ions can be expected to conspicuously decrease conformational fluctuations because they permeate the pore only slowly (cf. Frings *et al.* 1995).

References

Becchetti A, Gamel K & Torre V (1999). Cyclic nucleotide-gated channels. Pore topology studied through the accessibility of reporter cysteines. *J Gen Physiol* **114**, 377–392.

Benndorf K (1995). Low-noise recording. *Single-Channel Recording*, ed. Neher E & Sakmann B, pp. 129–145. Plenum Press, New York, London.

Benndorf K, Koopmann R, Eismann E & Kaupp UB (1999). Gating by cyclic GMP and voltage in the α subunit of the cyclic GMP-gated channel from rod photoreceptors. *J Gen Physiol* **114**, 477–489.

Bönigk W, Bradley J, Muller F, Sesti F, Boekhoff I, Ronnett GV, Kaupp UB & Frings S (1999). The native rat olfactory cyclic nucleotide-gated channel is composed of three distinct subunits. *J Neurosci* **19**, 5332–5347.

Bradley J, Reuter D & Frings S (2001). Nomenclature for ion channel subunits. *Science* **294**, 2095–2096.

Bucossi G, Nizzari M & Torre V (1997). Single-channel properties of ionic channels gated by cyclic nucleotides. *Biophys J* **72**, 1165–1181.

Chen T-Y, Peng Y-W, Dhallan RS, Ahamed B, Reed RR & Yau K-W (1993). A new subunit of the cyclic nucleotide-gated cation channel in retinal rods. *Nature* **362**, 764–767.

Doyle DA, Cabral JM, Pfuetzner RA, Kuo A, Gulbis JM, Cohen SL, Chait BT & MacKinnon R (1998). The structure of the potassium channel: Molecular basis of K^+ conduction and selectivity. *Nature* **280**, 69–77.

Finn JT, Grunwald ME & Yau K-W (1996). Cyclic nucleotide-gated ion channels: An extended family with diverse functions. *Annu Rev Physiol* **58**, 395–426.

Flynn GE & Zagotta WN (2001). Conformational changes in S6 coupled to the opening of cyclic nucleotide-gated channels. *Neuron* **30**, 689–698.

Frings S, Seifert R, Godde M & Kaupp UB (1995). Profoundly different calcium permeation and blockage determine the specific function of distinct cyclic nucleotide-gated channels. *Neuron* **15**, 169–179.

Gamel K & Torre V (2000). The interaction of Na^+ and K^+ in the pore of cyclic nucleotide-gated channels. *Biophys J* **79**, 2475–2493.

Gordon SE & Zagotta WN (1995). Localization of regions affecting an allosteric transition in cyclic nucleotide-activated channels. *Neuron* **14**, 857–864.

Hanke W, Cook NJ & Kaupp UB (1988). cGMP-dependent channel protein from photoreceptor membranes: single-channel activity of the purified and reconstituted protein. *Proc Natl Acad Sci U S A* **85**, 94–98.

Holmgren M (2003). Influence of permeant ions on gating in cyclic nucleotide-gated channels. *J Gen Physiol* **121**, 61–72.

Ildéfonse M & Bennett N (1991). Single-channel study of the cGMP-dependent conductance of retinal rods from incorporation of native vesicles into planar lipid bilayers. *J Membr Biol* **123**, 133–147.

Kaupp UB, Niidome T, Tanabe T, Terada S, Bönigk W, Stühmer W, Cook NJ, Kangawa K, Matsuo H, Hirose T, Miyata T & Numa S (1989). Primary structure and functional expression from complementary DNA of the rod photoreceptor cyclic GMP-gated channel. *Nature* **342**, 762–766.

Kaupp UB & Seifert R (2002). Cyclic nucleotide-gated ion channels. *Physiol Rev* **82**, 769–824.

Körschen HG, Illing M, Seifert R, Sesti F, Williams A, Gotzes S, Colville C, Müller F, Dosé A, Godde M, Molday L, Kaupp UB & Molday RS (1995). A 240 kDa protein represents the complete β subunit of the cyclic nucleotide-gated channel from rod photoreceptor. *Neuron* **15**, 627–636.

Liu J & Siegelbaum SA (2000). Change of pore helix conformational state upon opening of cyclic nucleotide-gated channels. *Neuron* **28**, 899–909.

Möttig H, Kusch J, Zimmer T, Scholle A & Benndorf K (2001). Molecular regions controlling the activity of CNG channels. *J Gen Physiol* **118**, 183–192.

Nizzari M, Sesti F, Giraudo MT, Virginio C, Cattaneo A & Torre V (1993). Single-channel properties of cloned cGMP-activated channels from retinal rods. *Proc R Soc Lond B Biol Sci* **154**, 69–74.

Root MJ & MacKinnon R (1994). Two identical noninteracting sites in an ion channel revealed by proton transfer. *Science* **265**, 1852–1856.

Ruiz ML & Karpen JW (1997). Single cyclic nucleotide-gated channels locked in different ligand-bound states. *Nature* **389**, 389–392.

Ruiz ML & Karpen JW (1999). Opening mechanism of a cyclic nucleotide-gated channel based on analysis of single channels locked in each liganded state. *J Gen Physiol* **113**, 873–895.

Sigworth FJ (1985). Open channel noise. I. Noise in acetylcholine receptor currents suggests conformational fluctuations. *Biophys J* **47**, 709–720.

Sun ZP, Akabas MH, Goulding EH, Karlin A & Siegelbaum SA (1996). Exposure of residues in the cyclic nucleotide-gated channel pore: P region structure and function in gating. *Neuron* **16**, 141–149.

Swenson RP & Armstrong CM (1981). K^+ channels close more slowly in the presence of external K^+ and Rb^+. *Nature* **291**, 427–429.

Taylor WR & Baylor DA (1995). Conductance and kinetics of single cGMP-activated channels in salamander rod outer segments. *J Physiol* **483**, 567–582.

Tränkner D, Jagle H, Kohl S, Apfelstedt-Sylla E, Sharpe LT, Kaupp UB, Zrenner E, Seifert R & Wissinger B (2004). Molecular basis of an inherited form of incomplete achromatopsia. *J Neurosci* **24**, 138–147.

Weitz D, Ficek N, Kremmer E, Bauer PJ & Kaupp UB (2002). Subunit stoichiometry of the CNG channel of rod photoreceptors. *Neuron* **36**, 881–889.

Zheng J, Trudeau MC & Zagotta WN (2002). Gating rearrangements in cyclic nucleotide-gated channels revealed by patch-clamp fluorometry. *Neuron* **28**, 369–374.

Zhong H, Molday LL, Molday RS & Yau K-W (2002). The heteromeric cyclic nucleotide-gated channel adopts a 3A:1B stoichiometry. *Nature* **420**, 193–198.

Zimmerman AL (1995). Cyclic nucleotide gated channels. *Curr Opin Neurobiol* **5**, 296–303.

Acknowledgements

We are indebted to U. B. Kaupp, Jülich, for providing the CNGA1 clone, to T. Zimmer and T. Baukrowitz for helpful discussions, and to T. Zimmer for preparing the RNA. We would also like to thank K. Schoknecht, S. Bernhardt, A. Kolchmeier, and B. Tietsch for excellent technical assistance. This work was supported by the Graduiertenkolleg 'Biomolekulare Schalter' and grant no. Be1250/14-2 of the Deutsche Forschungsgemeinschaft to K.B.